IMAGE DEHAZING GUIDED BY LOW-PASS REINFORCED AIRLIGHT

Codruta O. Ancuti *, *Cosmin Ancuti*†* *and Christophe De Vleeschouwer*†

* ETcTI, Universitatea Politehnica Timisoara, Romania
† ICTEAM, Universite Catholique de Louvain, Belgium

ABSTRACT

We introduce a simple but robust method to restore the visibility of hazy images. Our non deep-learning strategy refines a simplistic approximation of the airlight by taking advantage of the O-HAZE dataset that contains also the corresponding haze-free images. Knowing that the transmission is generally characterized by small values in hazy scenes, based on the optical model, we first assumes zero transmission, and approximate the airlight by the input hazy image. Then, using hazy and corresponding haze-free images available from the O-HAZE dataset, a second airlight estimate can be computed by solving the optical model assuming a simplified transmission map derived from dark channel prior. Observing that the difference between these two airlight estimates, primarily contains the low frequencies of the hazy image, we refine the airlight approximation derived from a zero transmission by reinforcing its low frequency component. We extensively tested our approach on real world hazy images. The qualitative and quantitative evaluations demonstrate that our approach yields better results than previous physically-based image dehazing techniques, and favorably compares with the deep learning dehazing approaches.

Index Terms— image dehazing, airlight, optical model

I. INTRODUCTION

Outdoor images are frequently altered by haze, which is a natural phenomenon resulting from the scattering and absorption of light by tiny particles suspended in the atmosphere. This can selectively attenuate the light spectrum, leading to decreased visibility, lost contrast, color artifacts and additional noise in the images. Consequently, restoring these images is crucial in various outdoor applications relying on visual appearance to (re-)identify objects [1], such as visual surveillance and automated driving assistance.

The mathematical nature of single image dehazing is ill-posed, mainly due to the fact that the haze's impact on each pixel varies and relies on the distance between the camera and the scene point. This relationship is commonly represented by the Koschmieder's light propagation model [2], which combines transmission and airlight to depict how haze affects the image captured.

Over the past few years, we have observed an important progress in the field of single image dehazing. In general existing methods are either physically-based techniques or deep learning-based techniques. The class of physically-based methods directly leverages the Koschmieder's optical model and depends on priors, such as dark channel prior [3], color lines [4] and color clusters [5]. For instance, the dark channel prior (DCP) assumes that the minimum intensity in RGB channels should be near zero in haze-free natural images. Various approaches have been considered to exploit DCP. Meng et al. [6] use a regularization strategy to refine the boundaries of the rough transmission estimated by DCP. Fattal [4] employs color-lines within the RGB color space to develop a technique that takes advantage of the one-dimensional structures found in the distributions of pixels within small patches of natural images. Berman et al. [5] extends [4] by noting that the RGB color space can be approximated by a discrete set of color clusters.

The class of deep learning techniques builds on convolution neural networks to learn the image prior [7], [8], [9], [10] or to learn the direct translation from hazy to clear images [11], [12], [13], [14]. DehazeNet, a convolutional neural network (CNN) approach developed by Cai et al. [8], aims to eliminate haze from images by training a model to convert hazy patches into clear ones. The process involves three steps: feature extraction, multi-scale mapping, and non-linear regression. To train the model, a synthesized dehazing dataset was utilized. Ren et al. [7] employ a coarse-scale network to estimate the transmission map, which is then further enhanced by a fine-scale network. AOD-Net [15] reformulates the optical model to produce the recovered images. GridDehazeNet [11] is composed of three primary modules. The initial module adapts the image representation to subsequent modules. The second module facilitates an effective exchange of information at varying scales. The final module refines the output by decreasing the prevalence of artifacts. The method of Zhang et al. [16] won IEEE CVPR NTIRE [17] image dehazing competition. It involves a Perceptual Pyramid Deep Network with an encoder-decoder architecture. The model is trained on paired data using a mix of mean squared error and perceptual losses.

Deep learning techniques [18], [19], [20], [21] have shown remarkable success for dehazing problem in the last years. This was due to the introduction of several specialized image dehazing datasets [22], [23], [24], [25], [26], [27], [28]. However, these databases are either synthetically generated [23], [26] or have a relatively small (e.g. tens) number of images [27], [28]. As a result the existing deep learning dahazing models often have trouble generalizing beyond the specific data (synthetic and realistic hazy images) they were trained on, leading to poor performance when tested on new real data.

In this paper we introduce a non-deep learning approach that is guided by a refined airlight approximation. In our approach we take advantage of the O-HAZE realistic dataset [27] (that contains also the corresponding haze-free image) to refine a simplistic approximation of the airlight. From our previous study [29] we know that the transmission is generally characterized by small values in hazy scenes, which allows to approximate the airlight by the input hazy image. Than, using hazy and corresponding haze-free images available from O-HAZE dataset, a second airlight estimate can be computed by solving the optical model using a transmission value derived from dark channel prior. Comparing these two airlight estimates we observe that their difference primarily contains the low frequencies of the hazy image. Hence, for images for which the haze-free image is not available, we propose to refine the airlight approximation derived from a zero transmission by reinforcing its low frequency component, thereby reducing its discrepancy with the airlight that would be computed from the haze-free image. Our method has been extensively tested on existing image dehazing datasets but also on real hazy images. The qualitative and quantitative evaluation demonstrates that our approach yields better results than the physically-based image dehazing techniques and favorably compares with the deep learning dehazing approaches.

II. OUR DEHAZING APPROACH

According to the *Koschmieder*'s [2] optical-model, the presence of atmospheric particles that absorb and scatter light along the observer's line of sight reduces the amount of reflected light and impacts the quality of the perceived visual image. Mathematically, the light intensity $\mathcal{I}$ of each pixel x, is expressed as:

$$\mathcal{I}(x) = \mathcal{J}(x) \; T(x) + A_\infty(x) \; [1 - T(x)] \tag{1}$$

where $\mathcal{J}$ represents the scene radiance or haze-free image that needs to be estimated, T is the transmission along the line of sight, and A_∞ represents the atmospheric light (airlight). The optical model expresses a linear relationship between observed image, image radiance, and airlight. The first term models how the scene radiance is reduced due to the properties of the atmosphere, while the *airlight* is the primary cause of image degradation in terms of color shifting, noise, and blur. Under homogeneous conditions, the transmission $T(x)$ is expressed as:

$$T(x) = e^{(-\beta \;\; d(x))} \tag{2}$$

where β is the attenuation coefficient of the medium due to scattering and $d(x)$ is the distance between the observer and the observed point.

In general, existing non-deep learning techniques estimate the two unknown parameters: transmission $T(x)$ and atmospheric light $A_\infty(x)$. Therefore, most solutions have to rely on prior knowledge such as dark channel priors [3], color lines [4], color clusters [5].

However, various assumptions such as considering that A_∞ (atmospheric light) is constant across the scene, have been demonstrated to fail for more complex hazy scenes, causing in general color shifting (see Figure 2).

To mitigate those limitations, our work takes advantage of the O-HAZE dataset [27] to refine a simplistic non-uniform approximation of the airlight. Our experiments clearly demonstrate the significant benefit resulting from this refinement. Regarding the transmission, our work follows previous works [3]. A reasonable approximation for the transmission of DCP is expressed as:

$$T(x) = (1 - \min_{R,G,B}(\mathcal{I}))^k \tag{3}$$

where k is a positive integer parameter that compresses the values of the transmission close to zero (here we generate the results using k=6).

In contrast to earlier works, the airlight is computed in a two step manner. The first step adopts the conventional observation made in previous studies [29] that the transmission is generally small in hazy scenes. Considering the extreme case, i.e. $T(x) = 0$, results in approximating A_∞ with $\mathcal{I}$. This approximation is denoted $A_{\infty 0}$ in the rest of the paper. The second step is the main contribution of our paper, and consists in refining the $A_{\infty 0}$ so as to improve the dehazed image. To design this refinement process, hazy and dehazed image pairs from the O-HAZE dataset have been considered to compute the airlight A_∞ resulting from Eq. 1 when $T(x)$ is approximated by Eq. 3 , while $\mathcal{I}(x)$ and $\mathcal{J}(x)$ correspond to the hazy and clean images available from the O-HAZE dataset, respectively.

Fig. 1. *Considering the hazy image (top-left), our refined airlight estimate $\bar{A}_\infty$ (top-right) shows a similar appearance with the original hazy image (since we basically filter out from the hazy image only few high frequencies). Using our zero-close transmission (Eq. 3) (bottom-left) we can solve the optical model and generate our dehazed result (bottom-right).*

Hence, it becomes possible to compare A_∞ and $A_{\infty 0}$ for the O-HAZE dataset pairs. As expected, this difference is very small and contains the low frequencies of the hazy image. Since the high frequencies of an image can be reconstructed by the sum of all its Laplacian values [30], we can express this difference mathematically as:

$$Diff_{\mathbf{A}} = A_{\infty 0} - \sum_{i=0}^{N} \mathcal{L}_i \tag{4}$$

where $\mathcal{L}_i$ is the i-th level of the Laplacian of the hazy image. In order to keep the solution computational efficient we set the value of N quite small (N=2), so basically only a few high frequencies of the image are filtered out. As a result, we can express our refined airlight estimate $\bar{A}_\infty$ by reinforcing its low-pass component through the addition of this difference. Mathematically our refined airlight estimate is expressed as:

$$\bar{A}_\infty = A_{\infty 0} + Diff_{\mathbf{A}} \tag{5}$$

Furthermore, because we have observed that the contribution of the low frequency hazy image in the airlight is increasing with the initial value of T , we have finally approximated the airlight using a formula inspired from alpha blending:

$$\bar{A}_\infty = (1 - T)^\alpha A_{\infty 0} + T^\alpha Diff_{\mathbf{A}} \tag{6}$$

where $A_{\infty 0}$ is computed for $T = 0$ and is identified with the hazy image, T is the transmission computed with the expression described in Eq.3, and the parameter α controls the amount of blending (default value is α=0.5). To restore the hazy images, we solve the optical model equation (Eq. 1) by using our final airlight estimate, $\bar{A}_\infty$, and the estimated transmission expressed by Eq. 3.

Fig. 2. *Qualitative comparison of dehazing methods [3], [6], [4], [5], [8], [7], [31] and our method for 5 images of the O-HAZE dataset.*

	He et al.			**Meng et al.**			**Fattal**			**Berman et al.**			**Dehaze-Net**			**Multiscale CNN**			**PMS Net**			**Ours**		
	SSIM	PSNR	CIEDE	SSIM	PSNR	CIEDE	SSIM	PSNR	CIEDE	SSIM	PSNR	CIEDE	SSIM	PSNR	CIEDE	SSIM	PSNR	CIEDE	SSIM	PSNR	CIEDE	SSIM	PSNR	CIEDE
Set 6	0.74	16.68	19.00	0.78	20.71	11.44	0.73	15.16	21.89	0.77	17.11	12.68	0.59	15.32	16.16	0.72	17.54	13.20	0.73	19.36	11.58	0.77	19.26	11.15
Set 10	0.78	16.22	15.22	0.76	15.98	16.63	0.75	16.42	17.49	0.72	14.48	17.77	0.71	15.02	16.17	0.80	16.57	13.70	0.77	16.80	12.29	0.76	18.34	12.78
Set 21	0.69	16.78	27.50	0.78	19.80	21.13	0.63	16.10	28.25	0.72	15.90	20.54	0.71	16.37	19.49	0.73	17.14	20.26	0.80	19.33	15.98	0.78	21.29	12.94
Set 30	0.75	15.71	18.85	0.74	14.68	18.59	0.72	14.68	18.46	0.81	17.48	14.55	0.77	18.57	12.70	0.82	19.72	12.66	0.78	19.94	12.17	0.88	23.02	8.15
Set 33	0.76	18.96	18.54	0.74	18.01	15.84	0.76	17.28	17.86	0.66	16.37	19.39	0.81	17.87	14.61	0.88	22.61	10.87	0.84	20.19	12.03	0.88	20.06	9.29
Average	0.74	16.59	20.75	0.75	17.44	16.97	0.71	15.64	19.85	0.75	16.61	17.09	0.67	16.21	17.35	0.77	19.07	14.67	**0.81**	19.05	13.47	**0.81**	**20.27**	**10.56**

Table I. **Quantitative evaluation.** *We compute the SSIM, PSNR and CIEDE2000 for the entire O-HAZE dataset. Besides the average value over the entire dataset in this table are presented also the results of the evaluated methods (from left to right [3], [6], [4], [5], [8], [7], [31] and our method) for the 5 images of the O-HAZE dataset that are shown in Figure 2.*

III. RESULTS AND DISCUSSION

We validate our approach by a comprehensive qualitative and quantitative evaluation. We first consider the realistic dehazing dataset O-HAZE [27] that contains 45 various outdoor scenes with haze generated with a professional haze machine that yields realistic hazy conditions. O-HAZE has the advantage to provide also the haze-free (ground-truth) corresponding images that allow to objectively evaluate the dehazing methods using traditional metrics. Table I presents the objective evaluation of the O-HAZE dataset based on several traditional image quality metrics (e.g. PSNR, SSIM [32] and CIEDE2000 [33], [34]). Besides the average value over the entire dataset, Table I also presents also the results of the evaluated methods (from left to right [3], [6], [4], [5], [8], [7], [31] and our method) for the 5 images of the O-HAZE dataset that are shown in Figure 2.

Moreover, in order to have a fair comparison with deep learning techniques, Figure 3 shows the results only for the last five images (the other 40 sets of images have been used for training the CNN models) of the O-HAZE, dataset, as recommended by the image dehazing challenge [17]. Table II provides the quantitative metrics for three deep-learning techniques [8], [31], [16] and three non deep-learning techniques [3], [5] (and our approach) when considering the 5 images shown in Figure 3.

Analyzing these results we can conclude that our approach performs better than the non-deep learning techniques but also yields comparable results with considered deep learning techniques. Obviously, being trained on O-HAZE dataset, the method of [16] yields the best results in terms of quantitative and qualitative evaluation. However, our approach approach performs closely and has the advantage of having a lower computational complexity compared with deep learning techniques.

In our evaluation we have also considered real world hazy images (see Figure 4). The results obtained on those images demonstrate that, in general our approach is able to properly recover the color and scene details. Moreover, compared to deep learning techniques, our technique method offers good generalization capabilities, and is able to better recover the details from distant regions (near the horizon).

To conclude, our approach is based on the observation that the transmission in hazy scenes is typically characterized by small values. Taking advantage of the O-HAZE dataset that contains also the corresponding haze-free images, we compute a refined airlight approximation derived from a zero transmission by enhancing its low-frequency component. As demonstrated by both qualitative and quantitative evaluations our our approach outperforms physically-based image dehazing methods and is comparable to deep learning-based dehazing methods.

Acknowledgments: *Part of this work was supported by a grant of the Ministry of Research, Innovation and Digitization, CCCDI - UEFISCDI, project number PN-III-P2-2.1-PED-2021-1572, within PNCDI III. Part of this work was supported by European Marie Skvodowska-Curie Individual Fellowships H2020-MSCA-IF-2019.*

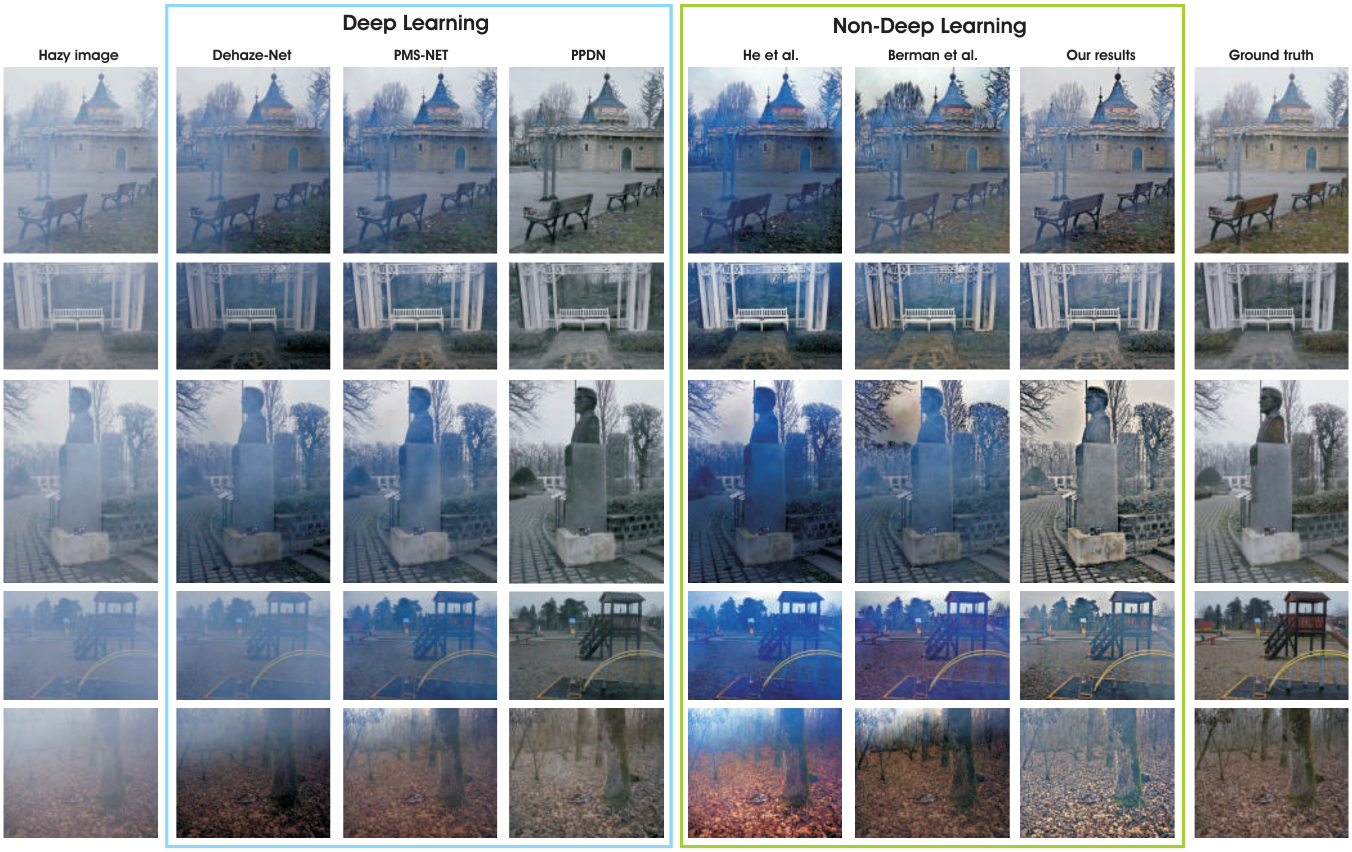

Fig. 3. *Comparison of the the deep-learning techniques [8], [31], [16] and non deep-learning techniques [3], [5] (and our approach) for the 5 images of O-HAZE that have been used in the image dehazing NTIRE challenge [17].*

	Dehaze-Net	PMS-Net	PPDN	He et al.	Berman et al.	Ours
SSIM	0.704	0.822	**0.861**	0.77	0.805	**0.833**
PSNR	17.245	19.322	**24.029**	16.871	17.655	**21.186**
CIEDE2000	15.081	13.112	**7.124**	18.963	14.519	**9.797**

Table II. *Quantitative results (shown in Figure 3) for the 5 images of O-HAZE that have been used in the image dehazing NTIRE challenge [17].*

Fig. 4. *Dehazing results obtained on real world hazy images. We compare with the methods (from left to right) of He et al. [3], Fattal [4], Berman et al. [5], Dehaze-Net [8] and PPDN [16].*

IV. REFERENCES

[1] Vladimir Somers, Christophe De Vleeschouwer, and Alexandre Alahi, "Body part-based representation learning for occluded person re-identification," in *IEEE Winter Conference on Applications of Computer Vision*, 2023.

[2] H. Koschmieder, "Theorie der horizontalen sichtweite," in *Beitrage zur Physik der freien Atmosphare*, 1924.

[3] K. He, J. Sun, and X. Tang, "Single image haze removal using dark channel prior," *IEEE Trans. on Pattern Analysis and Machine Intell.*, 2011.

[4] Raanan Fattal, "Dehazing using color-lines," *ACM Trans. on Graph.*, 2014.

[5] D. Berman, T. Treibitz, and S. Avidan, "Non-local image dehazing," *IEEE Intl. Conf. Comp. Vision, and Pattern Recog*, 2016.

[6] G. Meng, Y. Wang, J. Duan, S. Xiang, and C. Pan, "Efficient image dehazing with boundary constraint and contextual regularization," *In IEEE Int. Conf. on Computer Vision*, 2013.

[7] W. Ren, S. Liu, H. Zhang, X. Cao J. Pan, and M.-H. Yang, "Single image dehazing via multi-scale convolutional neural networks," *Proc. European Conf. Computer Vision*, 2016.

[8] B. Cai, X. Xu, K. Jia, C. Qing, and D. Tao, "Dehazenet: An end-to-end system for single image haze removal," *IEEE Transactions on Image Processing*, 2016.

[9] He Zhang and Vishal M. Patel, "Densely connected pyramid dehazing network," in *IEEE Conference on Computer Vision and Pattern Recognition (CVPR)*, 2018.

[10] Cong Wang, Yuexian Zou, , and Zehan Chen, "ABC-NET: Avoiding blocking effect and color shift network for single image dehazing via restraining transmission bias," in *IEEE ICIP*, 2020.

[11] Xiaohong Liu, Yongrui Ma, Zhihao Shi, and Jun Chen, "Griddehazenet: Attention-based multi-scale network for image dehazing," in *IEEE ICCV*, 2019.

[12] Xu Qin, Zhilin Wang, Yuanchao Bai, Xiaodong Xie, and Huizhu Jia, "FFA-Net: Feature fusion attention network for single image dehazing," in *In AAAI Conference on Artificial Intelligence*, 2020.

[13] Zhuoran Zheng, Wenqi Ren, Xiaochun Cao, Xiaobin Hu, Tao Wang, Fenglong Song, and Xiuyi Jia, "Ultra-high-definition image dehazing via multi-guided bilateral learning," in *IEEE Conference on Computer Vision and Pattern Recognition (CVPR)*, 2021.

[14] Xiaoqin Zhang, Jinxin Wang, Tao Wang, and Runhua Jiang, "Hierarchical feature fusion with mixed convolution attention for single image dehazing," *IEEE Transactions on Circuits and Systems for Video Technology*, 2022.

[15] Boyi Li, Xiulian Peng, Zhangyang Wang, Jizheng Xu, and Dan Feng, "AOD-Net: All-in-one dehazing network," in *IEEE ICCV*, 2017.

[16] H. Zhang, V. Sindagi, and V. M. Patel, "Multi-scale single image dehazing using perceptual pyramid deep network," *IEEE CVPRW*, 2018.

[17] C. Ancuti, C. O. Ancuti, R. Timofte, L. Van Gool, and L. Zhang et al., "Ntire 2018 challenge on image dehazing: Methods and results," *IEEE CVPR, NTIRE Workshop*, 2018.

[18] R. Liu, L. Ma, Y. Wang, and L. Zhang, "Learning converged propagations with deep prior ensemble for image enhancement," *IEEE Trans. Image Proc.*, 2019.

[19] Hang Dong, Jinshan Pan, Lei Xiang, Zhe Hu, Xinyi Zhang, Fei Wang, and Ming-Hsuan Yang, "Multi-scale boosted dehazing network with dense feature fusion," in *IEEE Conference on Computer Vision and Pattern Recognition (CVPR)*, 2020.

[20] Haiyan Wu, Yanyun Qu, Shaohui Lin, Jian Zhou, Ruizhi Qiao, Zhizhong Zhang, Yuan Xie, and Lizhuang Ma, "Contrastive learning for compact single image dehazing," in *IEEE Conference on Computer Vision and Pattern Recognition (CVPR)*, 2021.

[21] Chun-Le Guo, Qixin Yan, Saeed Anwar, Runmin Cong, Wenqi Ren, and Chongyi Li, "Image dehazing transformer with transmission-aware 3d position embedding," in *IEEE Conference on Computer Vision and Pattern Recognition (CVPR)*, 2022.

[22] J.-P. Tarel, N. Hauti, L. Caraffa, A. Cord, H. Halmaoui, and D. Gruyer, "Vision enhancement in homogeneous and heterogeneous fog," *IEEE Intelligent Transportation Systems Magazine*, 2012.

[23] C. Ancuti, C. O. Ancuti, and Christophe De Vleeschouwer, "D-hazy: A dataset to evaluate quantitatively dehazing algorithms," *IEEE ICIP*, 2016.

[24] Julia Luthen, Julian Wormann, Martin Kleinsteuber, and Johannes Steurer, "A rgb/nir data set for evaluating dehazing algorithms," *Electronic Imaging*, 2017.

[25] Yanfu Zhang, Li Ding, and Gaurav Sharma, "Hazerd: an outdoor scene dataset and benchmark for single image dehazing," *IEEE ICIP*, 2017.

[26] Boyi Li, Wenqi Ren, Dengpan Fu, Dacheng Tao, Dan Feng, Wenjun Zeng, and Zhangyang Wang, "Reside: A benchmark for single image dehazing," *IEEE Transactions on Image Processing*, 2018.

[27] C. O. Ancuti, C. Ancuti, C. De Vleeschouwer, and R. Timofte, "O-haze: a dehazing benchmark with real hazy and haze-free outdoor images," *IEEE CVPR, NTIRE Workshop*, 2018.

[28] C. Ancuti, C. O. Ancuti, M. Sbert, and R. Timofte, "Dense-Haze: A benchmark for image dehazing with dense-haze and haze-free images," *IEEE ICIP*, 2019.

[29] C. O. Ancuti, C. Ancuti, C. De Vleeschouwer, and A. C. Bovick, "Day and night-time dehazing by local airlight estimation," in *IEEE Transactions on Image Processing*, 2020.

[30] C. O. Ancuti, C. Ancuti, C. De Vleeschouwer, and A.C. Bovik, "Single-scale fusion: An effective approach to merging images," *IEEE Transactions on Image Processing*, 2017.

[31] Wei-Ting Chen, Jian-Jiun Ding, and Sy-Yen Kuo, "PMS-NET: Robust haze removal based on patch map for single images," in *IEEE CVPR*, 2019.

[32] Z. Wang, A. C. Bovik, H. R. Sheikh, and E. P. Simoncelli, "Image quality assessment: From error visibility to structural similarity," *IEEE Transactions on Image Processing*, 2004.

[33] G. Sharma, W. Wu, and E. Dalal, "The ciede2000 color-difference formula: Implementation notes, supplementary test data, and mathematical observations," *Color Research and Applications*, 2005.

[34] S. Westland, C. Ripamonti, and V. Cheung, "Computational colour science using matlab, 2nd edition," *Wiley*, 2012.